Comparison of Hysteresis Models for Nonlinear Dynamic Analysis of Structural Systems

Arya Bharath T K.[1*] and Nisha A.S.[2]

[1]M Tech (Structures) student, Department of Civil Engineering, NSS College of Engineering, Palakkad, Kerala
[2]Assistant Professor, Department of Civil Engineering, NSS College of Engineering, Palakkad, Kerala

*Corresponding author: aryabharath1995@gmail.com

ABSTRACT

Hysteresis is a non-linear phenomenon exhibited by the mechanical systems. Beyond elastic limit the loading and unloading path of most of the system will differ and that nonlinear path is indicated by hysteresis. The reason for shape of hysteretic cure may due to either changes in material properties beyond the elastic range or due to the changes in structural geometry because of subjected load. This response is a function of both immediate deformation and the previous residual deformation acted on it since it represents the dissipated energy of structure. The hysteretic characteristics or degrading characteristics includes pinching, stiffness degradation, load deterioration, and sliding. A study of four commonly available hysteresis models, which are Bouc Wen Model, Mostaghel Model, Menegotto Pinto Model and Preisach Model were briefly reviewed and discussed in this section and the outcome of this study is the best fitted model for the nonlinear analysis. The scope of the work is to simulate nonlinear response of the building frame subjected to earthquake excitation in a most effective way.

Keywords: Hysteresis Models, nonlinear analysis

1   Introduction

Under dynamic loading most of the structure will behave nonlinearly. Bouc Wen Model, Mostaghel Model, Menegotto Pinto Model and Preisach Model are some models which describes the hysteretic behavior in different field of applications. The aim of this paper is to select the most fitting model to simulate nonlinear response of the building frame subjected to earthquake excitation. The response of structure involves hysteretic characteristics or degrading characteristics which are pinching, stiffness degradation, load deterioration, and sliding.

i.   Pinching: Pinching is the progressive reduction in the rotational stiffness caused by closure of crack or rivet slip. This was commonly found in masonry and concrete structural systems and this can be represented in hysteresis by the reduction in area of hysteretic curve.

ii.   Stiffness Degradation: Stiffness degradation is the degradation of stiffness because of cyclic loading and this can be represented in hysteresis by the progressive reduction in the slop of curve.

iii. Load Deterioration: Load deterioration is the deterioration of the strength in a structural system when it is loaded to the same the displacement position. This can be represented by subsidence of peak in hysteretic curve.

iv.   Sliding: Excessive plastic deformations occurred in structural components such as connections and lateral bracing elements will leads to sliding of system. This also occurs as a result of cracking and tearing of elements. It is a function of dissipated energy of structure.

2   The Bouc-Wen Model

Bouc (1967) suggested a smoothly varying hysteresis model for single-degree-of-freedom (SDOF) system under cyclic loading. Baber and Wen extended the model with inclusion of stiffness and strength degradation which were defined as functions of dissipated hysteretic energy. Baber and Noori (1985) further incorporated pinching effect, which is a sudden loss of stiffness related to the opening and closing of cracks. This model has six shape parameters to describe the asymmetric hysteresis. The equation of motion for the single-degree-of-freedom (SDOF) system is explained as,

$m\ddot{u}(t) + c\dot{u}(t) + F_t[u(t),z(t),t] = F(t), \quad \dot{u}(0)=\dot{u}_0, \, u(0)=u_0$

where, $u(t)$ is the relative displacement of the mass m with respect to ground motion; c is the linear viscous damping coefficient; $F_t[u(t),z(t),t]$ is the non-damping restoring force which includes linear restoring force as $\alpha k u(t)$ and nonlinear restoring force as $(1-\alpha)kz(t)$; α (stiffness ratio) is the ratio of postyield slope of hysteretic loop to the pre-yield slope of the hysteretic loop, $z(t)$ is the displacement governed by the hysteretic spring; $F(t)$ is the time varying forcing function. Figure 1 shows the schematic diagram of mass m with Bouc-Wen model.
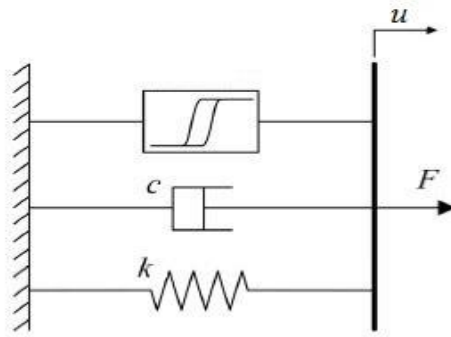
Figure 1. Schematic diagram of Bouc-Wen model [2]

The relation between $z(t)$ and $u(t)$ can be governed by the following equation

$\dot{z}(t) = \dfrac{h(z)}{\eta} (A\dot{u}(t) - \nu(\beta|\dot{u}(t)| \, |z(t)|^{n-1}z(t) + \gamma \, \dot{u}(t) \, |z(t)|^n)), \quad z(0) = z_0$

where, A signifies the tangent stiffness, it is generally kept as unity; β, γ and n are hysteretic shape parameters which control the shape of loading and unloading paths of the loop; ν and η are the strength and the stiffness degradation parameters, respectively, which are an increasing function of hysteretic energy and $h(z)$ is the pinching function.

2.1   Strength and Stiffness Degradation

Strength degradation (ν): This effect can be pictured as a downward shift of peak stress or load carrying capacity. Defined as follows,

$$\nu(\epsilon(t)) = 1 + \delta_\nu \epsilon(t)$$

Stiffness degradation (η): This is the increasing function of hysteretic energy and defined as follows,

$$\eta(\epsilon(t)) = 1 + \delta_\eta \epsilon(t)$$

where, $\epsilon(t)$ is the hysteretic energy. δ_v and δ_η represents the strength and stiffness degradation rates respectively. Both hysteretic force and hysteretic stiffness will degrade as δ_η increase whereas increase of δ_v reduces the hysteretic force keeping the hysteretic stiffness as constant.

2.2 Pinching Function

This effect can be depicted as the reduction in the area of hysteretic curve. The pinching function can be expressed as follows

$$h(z) = 1\text{-}\varsigma_1 \exp\left\{\frac{-(z(t)\text{sign}(\dot{u}(t)) - qzmax)}{\varsigma_2 2}\right\}.5$$

where, $\varsigma_1(\epsilon)$ determines the severity of pinching with values ranging from 0 to 1; the parameter $\varsigma_2(\epsilon)$ causes spread in the pinched region; q makes the level of pinching as a fraction of z_{max}.

2.3 Complete Model

The analytical form of complete hysteresis model can be represented as follows:

$$\ddot{u} + 2\,\xi_0\,\omega_0\,\dot{u} + a\,\omega_0{}^2\,u + (1\text{-}a)\,\omega_0{}^2\,z = f(t)$$

$$\dot{z} = \left\{1 - \zeta_s(1 - e^{-p\varepsilon})e^{-\left(zsgn(\dot{u}) - q\left[\frac{1}{(1+\delta v\varepsilon)(\beta+\gamma)}\right]^{\frac{1}{n}}\right)^2 / (\psi+\delta_\psi\varepsilon)^2 [\lambda+\zeta_s(1-e^{-p\varepsilon})]^2}\right\} \times$$

$$\left\{\frac{\dot{u} - (1+\delta v\varepsilon)(\beta|\dot{u}||z|^{n-1}z + \gamma\dot{u}|z|^n)}{(1+\delta\eta\varepsilon)}\right\}$$

$$\varepsilon(t) = (1-\alpha)\omega_0^2 \int_0^t z(u,t).\dot{u}(t).dt$$

Where ζ_s measures total slip; δ_ψ describes desired rate of pinching spread; the parameter, ψ controls the amount of pinching; p is the constant related to the rate of initial drop in slope and the parameter, λ controls rate of change of ς_2 with change of ς_1. ξ_0 linear viscous damping ratio and ω_0 pre-yield natural frequency of system.

RC non-seismic detailed interior beam–column joint specimens, Unit 1 and Unit 2 are tested under cyclic loading by Liu et al. [4]. Based on experimental results conducted on reinforced concrete (RC) interior and exterior beam–column joints with limited transverse reinforcement, an analytical Bouc – Wen model was formulated by Piyali Sengupta et.al [11]. A Comparison is made by Piyali Sengupta et.al [11] between the experimental and analytical shear force and horizontal deflection. The plots are shown in Fig.2. It is clear from the figure that both experimental and analytical results are fitting to each other and somewhere the analytical results are coinciding with experimental value.
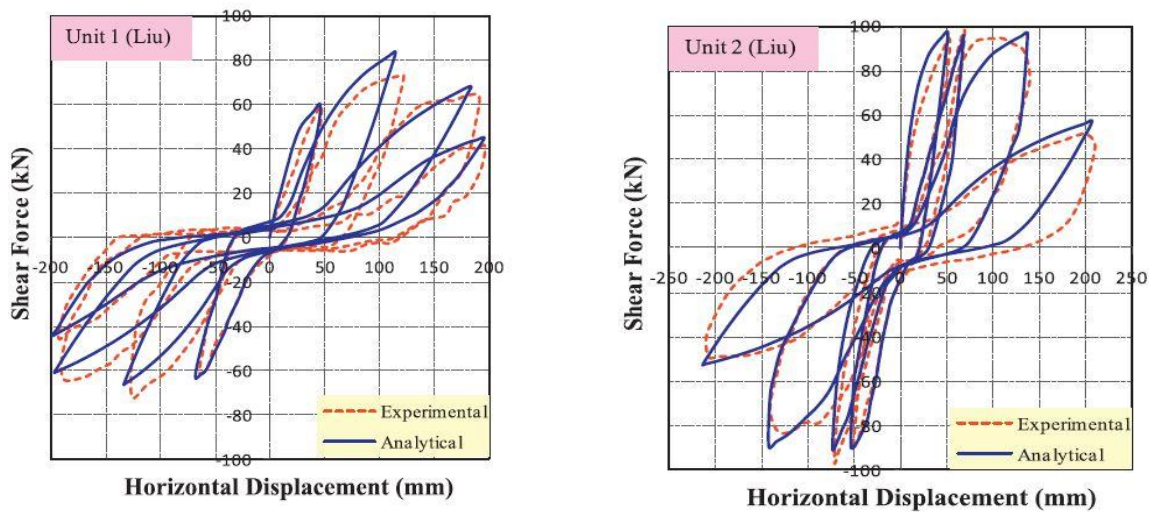
Figure 2. Analytical and experimental shear force versus horizontal deflection plots of Unit 1 and Unit 2 [11]

3 The Mostaghel Model

The analytical Mostaghel model also effectively describes general hysteretic behavior of structural systems. This model was formulated by Mostaghel (1999) includes the effects of pinching, sliding, strength and stiffness degradation. Figure 3(a) is the schematic diagram representing the model. The equation of motion representing a single-degree-of-freedom (SDOF) system is as follows

$$m\ddot{u}(t) + c\dot{u}(t) + F_T[u(t), z(t), t] = F(t), \dot{u}(0) = \dot{u}0, u(0) = u0$$

where, u is the deformation of the linear spring which is directly connected to the mass m, shown in Figure 3 (a) ; c describes the linear viscous damping coefficient; $F_T[u(t), z(t), t]$ is the non-damping restoring force (includes both linear restoring force and nonlinear restoring force which are $\alpha ku(t)$ and $(1-\alpha)kz(t)$ respectively); α represents stiffness ratio; $z(t)$ is the deformation of the hysteretic spring connected to a slider ; F(t) is the time varying forcing function.
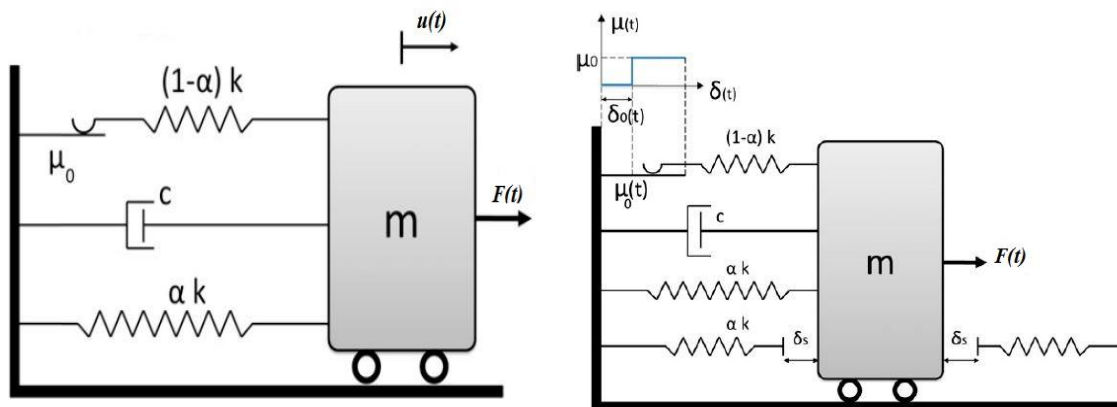
Figure 3. (a) SDOF system describing Mostaghel's model, (b) Modified SDOF system including gap element, additional stiffness and variable μ in slider [7].

3.1 Pinching Function

Mostaghel (1999) has defined two types of pinching,

i. Strength pinching: This effect is a result of strength unequalness for loading in opposite directions. Here the yield force $k\delta$ changes to $\lambda p\ k\delta$, where λp is the resistance ratio which ranges from 0 to unity and $\gamma p = 1 - \lambda p$.

ii. Stiffness hardening: Reduction in the area of hysteretic curve when a system encounters an additional stiffness at higher levels of its response. This effect can be depicted by introducing additional elastic stiffness with an initial gap δs, which is placed symmetrically to the mass as shown in Figure 3(b).

3.2 Stiffness and Strength Degrading System

From relation, $\mu m g = (1 - \alpha)\ k\delta$, it is clear that μ is directly proportional to $k\delta$. The frictional coefficient being directly proportional to $k\delta$ will cause decrease in either k or δ. Stiffness degradation is incorporated by inducing decrease in stiffness of the system, k with δ being constant. Similarly, strength degradation is incorporated by decrease in yield displacement, δ, keeping k as constant.

a) Strength degradation function:

$$\phi_l(t) = \frac{1}{1 + \lambda_1\ \varepsilon(t)}, 0 < (t) < 1$$

b) Stiffness degradation function

$$\phi_k(t) = \frac{1}{1 + \lambda_k\ \varepsilon(t)}, 0 < (t) < 1$$

where $\varepsilon(t)$ represents the total hysteretic energy absorbed by the structural system; λ_l represents the strength degradation factor, $\lambda_l \geq 0$; λ_k represents the stiffness degradation factor, $\lambda_k \geq 0$.

3.3 Sliding System

In order to formulate a model which includes sliding, a new slider system with variable friction coefficient, $\eta(t)$, was introduced to the model as portrayed in Figure 3(b). This model consider the sliding as increasing phenomenon and the function of the friction coefficient $\eta(t)$ includes an ascending function $\delta_0(t)$ which represents the relative initial slackness in the slider for each cycle with a time span starting from zero. Thus $\eta(t)$ can be defined as the function of the slider's initial slackness, $\delta_0(t)$.

$$\eta(t) = \begin{cases} 0 & if\ \delta(t) < \delta_0(t) \\ \eta_0 & if\ \delta(t) > \delta_0(t) \end{cases}$$

3.4 Complete Model

The normalized final equation, including pinching, stiffness degradation, load deterioration, and sliding phenomena, is shown in figure 4 and can be expressed as follows:

$$\ddot{y}(\tau) + 2\xi\dot{y} + \alpha y(\tau) + \alpha_s(|\ y| - \gamma_s)sng(y)\bar{N}(|\ y| - \gamma_s) + (1 - \alpha)z = P_0 p(\tau)$$

$$\dot{z} = \dot{y}\phi_k\ \{N(\dot{y})\big[M(z - \lambda_p\phi_l)\bar{M}(y - \acute{\delta}_0) +\ M(z - \phi_l)\bar{N}(y - \acute{\delta}_0)\big]$$
$$+ M(\dot{y})\big[\bar{N}(z + \lambda_p\phi_l)N(y - \acute{\delta}_0) + \bar{N}(z + \phi_l)M(y - \acute{\delta}_0)\bar{M}(y + \acute{\delta}_0)\big]\}$$

$$\dot{\varepsilon}(t) = \phi_l(1-\alpha)|\,\dot{y}|\,\left[N(\dot{y})N(y-\gamma_p) + \bar{M}(\dot{y})M(y+\gamma_p) + \lambda_p\bar{N}(\dot{y})M(y) + \lambda_p M(\dot{y})N(y)\right].|\,1 -$$
$$\{\bar{N}(\dot{y})[\bar{M}(z-\lambda_p\phi_l)\bar{M}(y) + \bar{M}(z-\phi_l)\bar{N}(y)]\}$$

Where N, M, $\bar{N}$, and $\bar{M}$ are functions derived from the Signum function (Sgn) and hence which are non-differentiable.
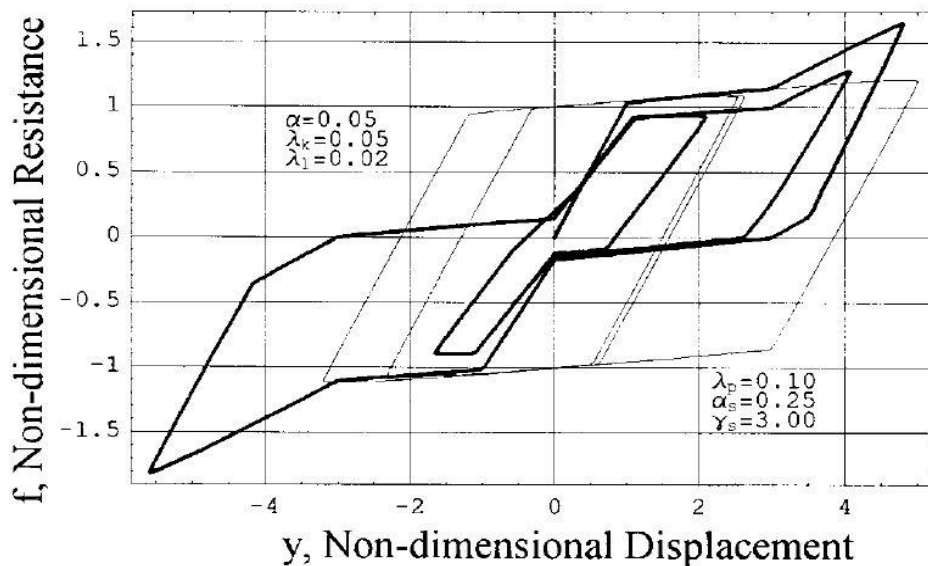
Figure 4. System Hysteretic loop with stiffness degradation, stiffness hardening, pinching and load deteriorating system [9].

For establishing the validity of the proposed Mostaghel model, the experimental results are cross checked with analytical results and the damage model which is implemented in the OpenSees environment. This was derived by considering both the concentrated rotation at the interfaces between the joint and adjacent beam-columns and the shear distortions in the joint panel. A comparisons proposed by Mojtaba Farrokh [8] between the proposed analytical model, the shear model, and the experimental results, considering the hysteretic energy, the area under the envelope curve, and the R2 factor (a comparative factor which determines accuracy). It is clear from the figure that experimental, analytical and OpenSees Models yields the results which are comparable but not as smooth as in Bouc-Wen Model.
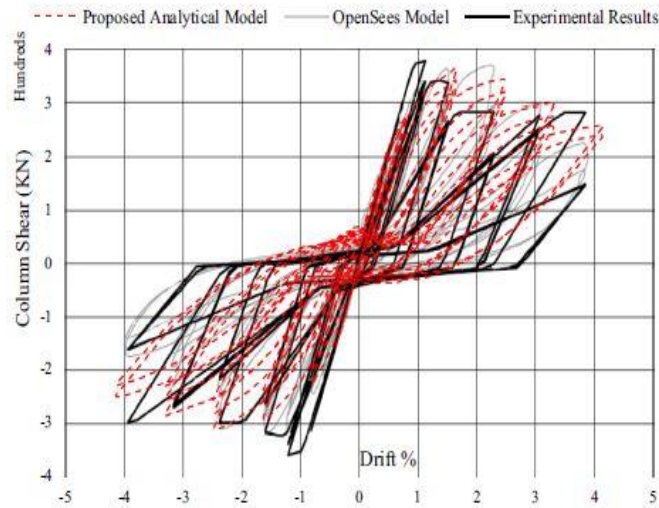
Figure 5. Comparison of proposed Mostaghel Model with experimental results and shear model [8]

4   Menegotto- Pinto Model

The model was proposed by Menegotto and Pinto which is a special plasticity model for the cyclic behavior of steel structures and joints. For joints moment rotation relationship is developed by Menegotto and Pinto. The model was initially programmed by Yassin (1994) based upon the stress strain relationship proposed by Menegotto and Pinto (1973), coupled with the isotropic hardening rules proposed by Filippou et al. (1983). This is found to be yet efficient. The general Menegotto-Pinto model (which is a uniaxial constitutive model) can be expressed as,

$$\sigma^* = b\varepsilon^* + \frac{(1-b)\varepsilon^*}{[1+\varepsilon^{*R}]^{1/R}}$$

Where σ^* and ε^* are the normalized stress and strain respectively. b is the strain hardening ratio; R is a parameter that controls the shape of the transition curve between the two asymptotes of elastic loading and postyield hardening branches. σ^* and ε^* can be defined as

$$\sigma^* = \frac{\sigma-\sigma_r}{\sigma_0-\sigma_r} \qquad and \qquad \varepsilon^* = \frac{\varepsilon-\varepsilon_r}{\varepsilon_0-\varepsilon_r}$$

where σ and ε are strain and stress, σ_0 and ε_0 are stress and strain at the intersection point of the two asymptotes, σ_r and ε_r are strain and stress at the previous strain reversal and R can be defined as

$$R = R_0(1 - \frac{cR_1\xi}{cR_2+\xi})$$

where R_0, cR_1 and cR_2 are experimentally determined parameters, ξ is the normalized plastic strain as defined as

$$\xi = \left| \frac{\varepsilon_p-\varepsilon_0}{\varepsilon_y} \right|$$

where ε_p and ε_y are plastic strain and yield strain, respectively. The stress shift for isotropic hardening in compression and tension can be represented by the following equation.

$$\sigma_{st} = \sigma_y a_1 \left(\frac{\varepsilon_p^{max}-\varepsilon_p^{min}}{2\,a_2\varepsilon_y}\right)^{.8} \qquad and \qquad \sigma_{st} = \sigma_y a_3 \left(\frac{\varepsilon_p^{max}-\varepsilon_p^{min}}{2\,a_4\varepsilon_y}\right)^{.8}$$

where a_1, a_2, a_3, and a_4 are experimentally determined model parameters and ε_y is the initial yield strain. ε_p^{max} and ε_p^{min} are minimum and maximum recorded strains in each loading cycles. The 10 model parameters in this model are E_0, σ_y, b, R_0, cR_1, cR_2, a_1, a_2, a_3, and a_4. E_0 corresponding to the postyield response.

The moment-rotation curves of the CDWJs (cruciform diaphragm welded joint) at Yujiapu railway station located in Tianjin, China, was predicted by the proposed mathematical model and they are compared with that from the numerical simulation as shown in Figure 6. The comparison shows that when the strength degradation is not considered, the accuracy of the proposed model is noted. The maximum value of the average percentage difference is only 3.04%. Hence, the Menegotto-Pinto model could be used to estimate the M-θ characteristic of CDWJ.
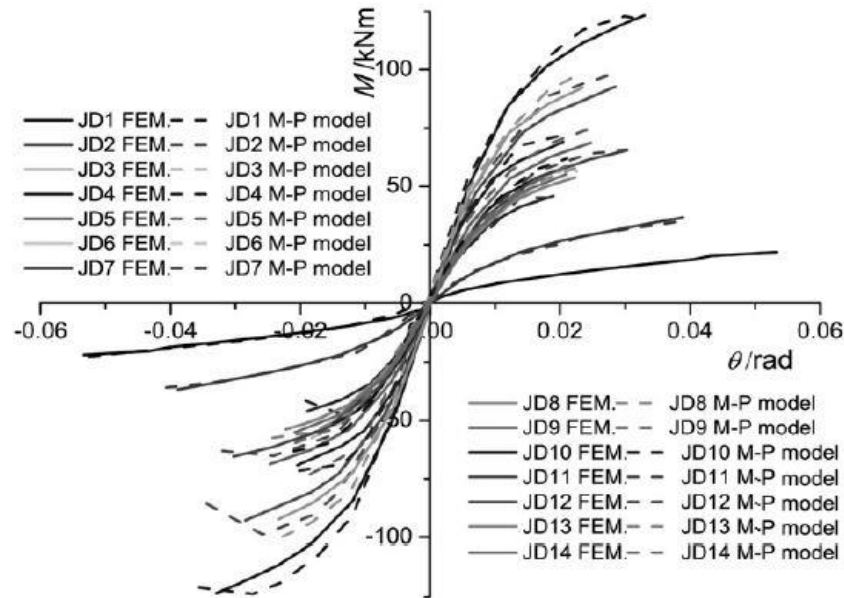
Figure 6. Comparison of hysteretic curves obtained from experiment and Menegotto- Pinto model [3]

5 Preisach Model

Preisach model is mainly concerned with hysteresis of smart materials such as ferroelastic, ferroelectric, ferromagnetic materials, and electroactive polymers. This model have five model parameters. The Preisach model is a rate-independent hysteresis model. Which determines the output signal y(t), through linear superposition of continuous operators applied to the input signal x(t) as follows, where t represents time.

$$y(t) = \int_0^{+\infty} \int_{-\infty}^{+\infty} \mu(r,s) R_{s-r,s+r} \, [x](t) \, dsdr$$

where $\mu(r,s)$ density function; and $R_{s-r,s+r}$ relay operator with mean value of s and half-width value of r. In this model the parameters are converted to operators. The three forms of the operators used in this model are Relay, Play and Stop as shown in Figure 7.
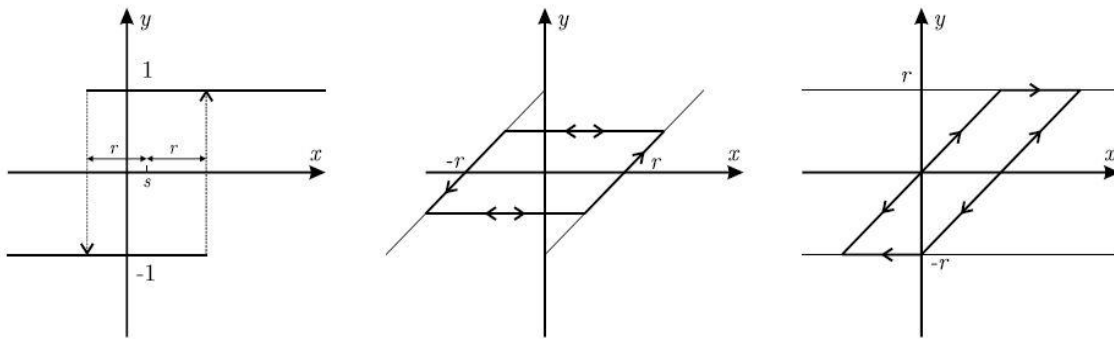
Figure 7. (a) relay, (b) play, (c) stop operator [8]

6   Conclusions

In this paper, four commonly available hysteresis models, which are Bouc Wen Model, Mostaghel Model, Menegotto Pinto Model and Preisach Model are compared in order to select best fitted model for dynamic analysis of oscillator or shear frame models and following conclusions were drawn:

- The Bouc –Wen and Mostaghel models incorporate hysteresis characteristics.
- The Bouc-Wen model has 12 model parameters, whereas Mostaghel model has 7 model parameters.
- The Bouc-Wen model is found to capture smooth hysteresis, whereas the Mostaghel model has non differentiable functions and hence the transition from elastic to inelastic regime is not smooth.
- The Menegotto-Pinto model is a special plasticity model for the cyclic behavior of steel and joints and it has 10 model parameters.
- Preisach model give highly accurate results in different fields of engineering such as electromagnetism, soil mechanics and shape memory alloys. But when this model used under structural system, it shows less accuracy.
- Bouc-Wen model and Mostaghel model are more accurate in capturing hysteretic characteristics of structural systems.

How to Cite this Article:

Arya Bharath TK., & Nisha, A. S. (2021). Comparison of Hysteresis Models for Nonlinear Dynamic Analysis of Structural Systems. *AIJR Proceedings*, 280-289.

References

1. Greg C. Foliente (1995). *Hysteresis modeling of wood joints and structural systems.* Journal of Structural Engineering, 121, 06.
2. Hongtao Zhu et.al. (2019). *An efficient parameters identification method of normalized Bouc-Wen model for MR damper.* Journal of Sound and Vibration, 448, 146–158.
3. Jihui Xing et.al. (2017). *In-plane bending hysteretic behavior of cruciform diaphragm welded joints with axial force.* Journal of Constructional Steel Research, 132 ,164–178.
4. Liu A, Carr AJ, Park R (2002). *Seismic assessment and retrofit of pre-1970s reinforced concrete frame structures.* University of Canterbury.
5. M. Bosco et.al. (2016). *Improvement of the model proposed by Menegotto and Pinto for steel*. Engineering Structures, 124,442–456
6. Mehran Zeynalian et.al (2018). *A New Displacement-Control Analytical Hysteresis Model for Structural Systems.* Int J Civ Eng, 16, 671–680.
7. Mehran Zeynalian et.al (2012). *Analytical Description of Pinching, Degrading, and Sliding in a Bilinear Hysteretic System*. J . Eng. Mech, 138,1381-1387.
8. Mojtaba Farrokh (2018). *Hysteresis Simulation Using Least-Squares Support Vector Machine.* J. Eng. Mech, 144(9): 04018084.
9. Naser Mostaghel (1999). *Analytical description of pinching, degrading hysteretic systems.* J. Eng. Mech, 125(2), 216-224.

10. Piyali Sengupta et.al *(2014). Hysteresis Behavior of Reinforced Concrete Walls*. Journal of Structural Engineering, 04014030

11. Piyali Sengupta et.al (2013). *Modified Bouc–Wen model for hysteresis behavior of RC beam–column joints with limited transverse reinforcement.* Engineering Structures, 46, 392–406.

12. Sung-Yong Kim et.al (2019). *Description of asymmetric hysteretic behavior based on the Bouc-Wen model and piecewise linear strength-degradation functions*. Engineering Structures, 181, 181–191.

13. Zhe Qu et.al. (2017).*Cyclic loading test of double K-braced reinforced concrete frame subassemblies with buckling restrained braces.* Engineering Structures, 139, 1–14.